Monte Carlo–Based Approach to Estimating Fragility Curves of Floating Docks for Small Craft Marinas

Adam S. Keen, S.M.ASCE[1]; Patrick J. Lynett, M.ASCE[2]; Martin L. Eskijian, M.ASCE[3]; Aykut Ayca, S.M.ASCE[4]; and Rick Wilson, A.M.ASCE[5]

Abstract: As a result of damage from the 2010 Chile and 2011 Japanese teletsunamis, tsunami risk to small craft marinas along the West Coast of the United States has become an important concern. This paper outlines an assessment tool that can be used to quantify the tsunami damage potential in small craft harbors. The methodology is based on the demand and capacity of a floating dock system and uses a Monte Carlo framework to address the uncertainty of input parameters. Detailed numerical modeling and damage calibration data from recent tsunamis are used to benchmark the approach. Results are provided as fragility curves and give a quantitative assessment of survivability. This tool yields an indication as to the survivability and/or failure of a floating dock system of vessels and floating components/piles subject to tsunami events. The objective of the presented effort is to quickly evaluate whether a floating dock is likely to survive or be destroyed by a particular tsunami scenario. **DOI: 10.1061/(ASCE)WW.1943-5460.0000385.** *© 2017 American Society of Civil Engineers.*

Introduction

Tsunamis pose a significant risk to the infrastructure located along the West Coast of the United States. Although the frequency of significant tsunami events is small compared with other natural hazards, the impact of tsunami events (especially to small craft harbors) is high. It is this interplay between frequency of events and resultant impact that drives the tsunami risk. For example, the 2011 tsunami from Japan caused over $100 million in damage to 27 harbors in California (Wilson et al. 2013). Following the damage resulting from the 2010 Chile and 2011 Japanese teletsunamis, significant efforts have been initiated to understand the mechanisms and potential scope of tsunami impacts in harbors (Lynett et al. 2012; Borrero et al. 2015). The State of California seeks to mitigate subsequent damage from the next major tsunami that might strike the Pacific Coast (Wilson et al. 2013).

Existing methodologies to predict damage to small craft harbors during tsunami events are limited. Approaches vary but the methodologies that do exist have largely been data driven, relying on correlations between input parameters and damage. For instance, using damage reports from the 2011 Tōhoku tsunami in Japan, Suppasri et al. (2014) derived independent loss functions for maximum tsunami surface elevation and maximum flow velocities using linear regression analysis assuming a logarithmic loss function. The loss functions showed good agreement with data, but their independence limited their applicability. Therefore, Muhari et al. (2015) extended the work of Suppasri et al. (2014) to developed new multivariate loss functions to estimate the potential damage of marine vessels based on a set of input parameters. The multivariate analysis coupled the input terms, which allowed for direct application to damage estimates. Using a semiquantitative approach, Lynett et al. (2014) compared damage assessments in five California harbors to high-resolution model results of maximum current speed to derive approximate damage limits to small craft harbors.

These data-driven loss functions are ideal for applications in which the engineer needs to directly estimate the functionality between independent and dependent variables to quickly assess hazards. However, mathematical correlations do not necessarily ensure physical significance, making it sometimes difficult to interpret the physics involved in the hazard assessment. For instance, processes such as surface elevation and current speed are commonly assumed to be the dominant terms that correlate with damage, whereas other inputs, such as current direction or vessel dimensions, are not. Well-established drag formulations, however, would tend to suggest that these additional terms would have some impact on the resultant damage. Unless these terms are added to the analysis (either directly or indirectly), the interaction would not be captured by the loss functions. Physics-based approaches complicate the methodology but are a necessary component to extend the community's understanding of the hazard.

In addition to the overall approaches, it is also important that the outputs from vulnerability models are practical and straightforward. Unlike flow models that output quantities like surface elevation or current speed (which is directly comparable from model to model), output quantities between vulnerability models often differ because the methodology and calibration are often dictated by the availability of damage data for discrete events. Although one model might output percentage loss, another outputs dollar value loss and another outputs loss intensity; intermodel comparisons are rarely performed. The output metrics between models are not directly comparable; therefore they are limited in their application. A generalized physics-based approach with generalized outputs is advantageous because it can be applied to a variety of scenarios.

[1]Gradute Student, Sonny Astani Dept. of Civil and Environmental Engineering, Univ. of Southern California, Los Angeles, CA 90089 (corresponding author). E-mail: adamkeen@usc.edu

[2]Professor, Sonny Astani Dept. of Civil and Environmental Engineering, Univ. of Southern California, Los Angeles, CA 90089. E-mail: plynett@usc.edu

[3]Senior Engineer, California State Lands Commission, Long Beach, CA 90802. E-mail: mleskijian@gmail.com

[4]Gradute Student, Sonny Astani Dept. of Civil and Environmental Engineering, Univ. of Southern California, Los Angeles, CA 90089. E-mail: ayca@usc.edu

[5]Senior Engineering Geologist, California Geological Survey, Sacramento, CA 95814. E-mail: rick.wilson@conservation.ca.gov

Note. This manuscript was submitted on March 24, 2016; approved on November 10, 2016; published online on February 9, 2017. Discussion period open until July 9, 2017; separate discussions must be submitted for individual papers. This paper is part of the ***Journal of Waterway, Port, Coastal, and Ocean Engineering***, © ASCE, ISSN 0733-950X.

This paper will outline a physics-based tool that can be used to assess the tsunami hazard to small craft harbors. The methodology is based on the demand and also the structural capacity of the floating dock system, which is composed of floating docks/fingers and moored vessels. Because of the uncertainties in the current direction, the exact current speed, and the remaining capacities of the floating structure, a Monte Carlo approach has been used. The equations used to determine the forces on the vessels and floating structure are taken from conventional sources, and the system of vessels, floating components, and piles are all included in the assessment. The condition of the floating dock structure is included, and a demand/capacity ratio is used as an index of failure. Results are provided as fragility curves and give a quantitative assessment of survivability. The derived fragility curves are validated by comparing them with the damage reports from the 2011 Tōhoku event in Santa Cruz Harbor, California. The fragility curves will be used by engineers to help analyze harbors in California and other regions to identify vulnerable sections of the harbors so that a predisaster mitigation function can be sought to make harbor improvements.

Statistical Methodology

Here, fragility curves for structural components in small craft harbors are estimated using Monte Carlo methodology. A Monte Carlo–based approach in structural analysis is a probabilistic tool in which the governing equations of motion or structural behavior might be well known but the independent variables of the input (i.e., current speed, current direction) as well as the structural capacities of the components (e.g., cleats, pile guides) might not be. The Monte Carlo approach requires a distribution of each input variable (usually with a rectangular-shaped, triangular-shaped, or Gaussian-shaped relationship) and then randomly samples each distribution within the described equations to generate a single computational result. The process repeats hundreds or thousands of times depending on the required accuracy and convergence of the system. A general outline of the procedure is show in Fig. 1. A fragility curve is estimated for each component and for each slip within the system that is likely to fail during a tsunami. The maximum failure probability from each component in all slips within the dock is then used to define the minimum capacity of the dock system. The approach is akin to essentially looking for the *weakest link* for each dock during a tsunami event. Neither cumulative damage nor damage that occurs from debris in the water impacting the boats and/or docks during the event is considered.

Data Requirements

Depending on the certainty of the parameter, inputs to the Monte Carlo model can be defined as either deterministic or probabilistic. Deterministic quantities are quantities that are known or are not expected to vary within a scenario. Regarding the floating docks, these include finger length, finger width, number of slips, number of piles, and number of cleats. Effectively, this implies that the analysis is performed as a damage assessment on the harbor as it exists presently; potential future change to the harbor layout might also be included in a probabilistic manner but will be addressed in future work. For this analysis within California, these quantities were estimated from historical high-resolution orthoimagery data available from the USGS.

In contrast to deterministic inputs, probabilistic inputs are those quantities that might not be exactly known but can be defined by a probability density function. These quantities would include current speed, current direction, water depth, seawater density, vessel length, vessel beam, and vessel draft. Each input variable was randomized assuming a rectangular probability density function (e.g., equal probability of any value within range) bounded by defined minima and maxima. Current speed and current direction were estimated from a high-resolution numerical model (to be discussed in more detail in later sections). Model results were finely sampled using the parameter surface to define the approximate minimum and maximum within the confines of each slip.

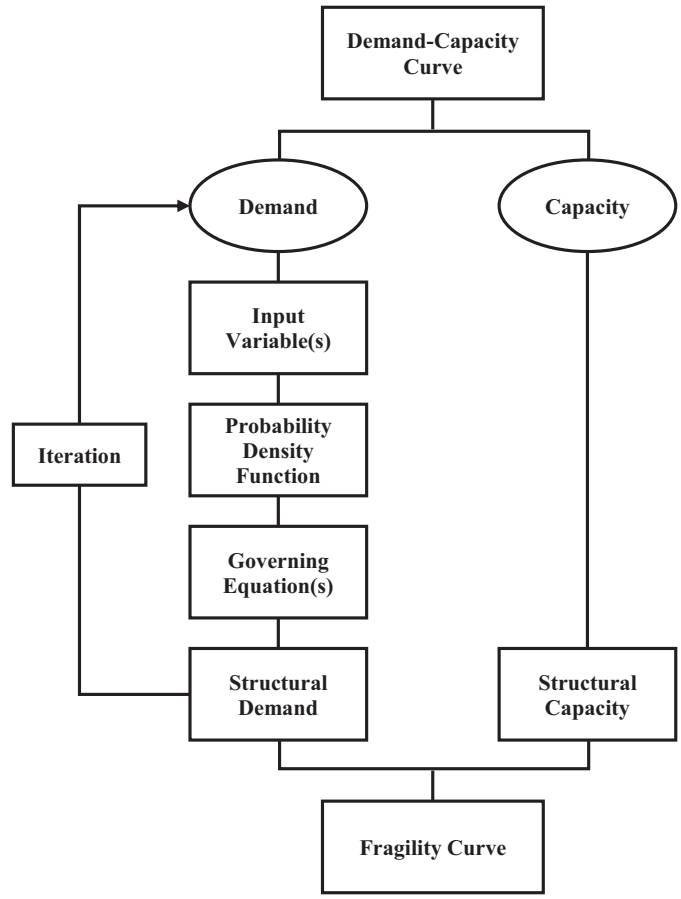

Fig. 1. General outline of the process used to define fragility curves based on a Monte Carlo–based demand-capacity analysis

Demand to Capacity Equations for Cleats

The governing equations for the transverse and longitudinal forces on vessels were used to calculate the *demand* from the tsunami current (U.S. Army Corps of Engineers 2005). The equations to determine the current forces on the vessels are summarized in this section. The approach is intended to be first order such that differential loads are not treated in this phase of the analysis.

For the transverse current forces on a vessel (U.S. Army Corps of Engineers 2005)

$$F_{yc} = \frac{1}{2}\rho_w \, V_c^2 \, L_{wl} \, T \, C_{yc} \sin\theta \tag{1}$$

where ρ_w = water density; V_c = current velocity; L_{wl} = length of the vessel at the waterline; T = vessel draft; C_{yc} = transverse drag coefficient; and θ = angle of velocity relative to the vessel longitudinal axis.

The transverse drag coefficient was estimated from (U.S. Army Corps of Engineers, 2005)

J. Waterway, Port, Coastal, Ocean Eng., 2017, 143(4): -1--1

$$C_{yc} = C_0 + (C_1 - C_0)\left(\frac{T}{d}\right)^2 \tag{2}$$

where C_0 = deepwater current drag coefficient for $T/d \approx 0$; C_1 = shallow water drag coefficient (= 3.2); and d = water depth. The deepwater drag coefficient can be estimated from

$$C_0 = 0.22\sqrt{\chi} \tag{3}$$

with χ defined as

$$\chi = \frac{L_{wl}^2\, A_m}{B\ V} \tag{4}$$

where A_m = immersed cross-sectional area of the vessel at midsection; B = maximum vessel beam at the waterline; and V = submerged volume of vessel.

Similarly, for the longitudinal current forces on the vessel, not considering propeller loads that could be highly variable (U.S. Army Corps of Engineers 2005)

$$F_{xc} = F_{x\ \mathrm{FORM}} + F_{x\ \mathrm{FRICTION}} \tag{5}$$

and

$$F_{x\ \mathrm{FORM}} = \frac{1}{2}\rho_w\ V_c^2\ B\ T\ C_{xcb}\cos\theta \tag{6}$$

where C_{xcb} = longitudinal current form drag coefficient $(= 0.1)$, and

$$F_{x\ \mathrm{FRICTION}} = \frac{1}{2}\rho_w\ V_c^2\ B\ S\ C_{xca}\cos\theta \tag{7}$$

where S = wetted surface area; and C_{xca} = longitudinal current skin friction coefficient. Here, the wetted surface area is estimated by

$$S = 1.7\ T\ L_{wl}^2 + \left(\frac{D}{T\ \gamma_w}\right) \tag{8}$$

where γ_w = weight density of water. The longitudinal current skin friction is a function of Reynold's number defined as

$$C_{xca} = \frac{0.075}{(\log_{10}\mathsf{R} - 2)^2} \tag{9}$$

where R = Reynolds number. For vessels, the Reynolds number is defined as

$$\mathsf{R} = \left|\frac{V_c\, L_{\mathrm{wl}}\cos\theta}{\nu}\right| \tag{10}$$

where ν = kinematic viscosity of water.

Vessels resist the tsunami demand via their cleat connection. An example of a cleat for Santa Cruz Harbor is shown in Fig. 2. The analysis presented here assumes that these cleats act as a system distributing the load evenly across the cleats. Small craft harbors within California typically secure each vessel within the slip using either a 2-cleat or 4-cleat configuration. These types of cleats are mounted on the dock with two bolts via a timber connection. By knowing the size and number of bolts, capacities for each cleat can be directly estimated. However, even if the exact configurations of the cleats are known for each slip, the governing in situ cleat *capacities* are nearly impossible to accurately quantify. Many harbors within California have aged and are not at their original, full capacity. Therefore, the results are presented with respect to the *required capacity*, which can be interpreted as the capacity needed to resist the tsunami demand.

Fig. 2. Typical cleat configuration for Santa Cruz Harbor (image by Adam S. Keen)

Fig. 3. Typical pile guide configuration for Santa Cruz Harbor (image by Adam S. Keen)

Demand to Capacity Equations for Pile Guides

The governing equations for the transverse and longitudinal forces on vessels were used to calculate the demand from the tsunami current on the floating dock system (U.S. Army Corps of Engineers 2005). The equations to describe the loads on the floating dock and fingers are the same as used for the vessels. One difference is that the angle for the dock is 90° out of phase from the vessels (perpendicular to the fingers/vessels); the fingers are in the same line (approach angle) as the vessels. Additionally, pulling forces from the cleats are assumed to have no effect on the pile guides.

Floating docks and fingers resist the tsunami demand via the pile guide. An example of a pile guide for Santa Cruz Harbor is shown in Fig. 3. For this analysis, forces on the pile guides are determined

J. Waterway, Port, Coastal, Ocean Eng., 2017, 143(4): -1--1

based on the demand equation. The demand is then averaged based on the number of pile guides to determine the load per pile guide. Multiple pile guides within a dock system resist horizontal loads while allowing the dock to adjust to a rising and falling tide. For the pile guide capacity, a typical pile collar in California consists of between four and eight bolts that connect to the dock via a timber connection. By knowing the size and number of bolts, capacities for each pile guide can be directly estimated. However, even if the exact configuration of pile guides by the dock is known, like the cleat capacities, it is nearly impossible to accurately quantify the in situ pile guide capacities. Therefore, like the cleat capacities, the results are presented with respect to the *required capacity*, which can be interpreted as the capacity needed to resist the tsunami demand.

Numerical Modeling of Tsunami Events

Santa Cruz Harbor is a small municipal harbor located along the Central California coast. The location of Santa Cruz Harbor is shown in Fig. 4. The harbor consists of two long and narrow basins that extend inland from the shoreline. The north and south basins were built nearly a decade apart, which resulted in differences in material construction between the two basins. The south basin was completed in 1963, and was originally built using timber deck materials and piles typical of the period. By the time the north basin was completed in 1972 floating dock construction had changed, favoring a more robust composite-type construction (Mesiti-Miller Engineering, Inc. 2011).

According to the Santa Cruz Port District website, Santa Cruz Harbor has space for approximately 1,000 wet-berthed and 275 dry-stored vessels. Roughly 15% of these vessels are commercial fishing boats, 35% pleasure power boats, and 50% pleasure sailboats (Santa Cruz Port District 2016). Of the approximately 800 wet slips, 35% of the vessels are within the ≤6.1-m range, 40% are within the 9.1-m range, 20% are within the 12.2-m range, and 5% are within the 15.2-m or greater range.

Since the harbor's completion, very few of the docks had been replaced leaving the harbor vulnerable to tsunami events. During the 2011 Tōhoku tsunami, a series of waves caused significant damage to Santa Cruz Harbor. Numerical models of two tsunami events were analyzed for Santa Cruz Harbor to assess the harbor's vulnerability using Monte Carlo methodology. One scenario was the 2011 Tōhoku tsunami, which damaged almost all docks within Santa Cruz Harbor. Another scenario was a hypothetical tsunami generated

Fig. 4. Location of Santa Cruz Harbor along California's Central Coast (Service Layer Credits: Esri, HERE, DeLorme, MapmyIndia, © OpenStreetMap contributors, and the GIS user community)

J. Waterway, Port, Coastal, Ocean Eng., 2017, 143(4): -1--1

by a large earthquake (magnitude 9.2) along the Alaska-Aleutian subduction zone (AASZ).

Hydrodynamic modeling for this study was conducted using the numerical model method of splitting tsunamis (MOST) (Titov and González 1997; Titov and Synolakis 1998). This model is capable of simulating the full development of the tsunami from wave generation to wave run-up. Tsunami propagation is modeled based on the elastic deformation theory (Okada 1985), whereas the inundation is modeled based on a derivation of the VTCS model (Titov and Synolakis 1998). The model has been extensively validated for a number of global scenarios. Variants of the MOST model have been in constant use for tsunami hazard assessments in California since the mid-1990s (Lynett et al. 2014). The reader is referred to Titov and González (1997) for further information on the model as well as general validation.

In this study, MOST is used to propagate tsunami waves from the source to the nearshore region, using a system of nested grids. The outermost grid at 4 arc-min resolution covers the entire Pacific Basin. Three additional grids of increasingly finer resolution were derived from data provided by the National Oceanic and Atmospheric Administration National Geophysical Data Center specifically for tsunami forecasting and modeling efforts (Grothe et al. 2012). The innermost nearshore grid has a 10-m resolution and takes boundary input from the previous MOST nested layer.

Although model predictions of surface elevation are commonly compared with tide gauge data, comparisons with current speed are less common, principally due to the lack of data. Therefore, the MOST modeling work for Santa Cruz Harbor was validated against the high-order Boussinesq-type model Cornell University Long and Intermediate Wave Modeling Package (COULWAVE) (Lynett et al. 2014). Model results suggest that although not as accurate as the higher order COULWAVE model, the MOST tsunami model satisfactorily reproduces measured tsunami-induced current speeds (Lynett et al. 2014).

A total of five events were modeled for Santa Cruz Harbor including two historical events and three realistic scenarios. The five events include the 2010 magnitude 8.8 Chile event (historical), a magnitude 9.0 Cascadia scenario, the 2011 magnitude 9.0 Japan event (historical), a magnitude 9.4 Chile North scenario, and a magnitude 9.2 Eastern Aleutian-Alaska scenario. A summary of these five events is shown in Fig. 5. Two events, the 2011 magnitude 9.0

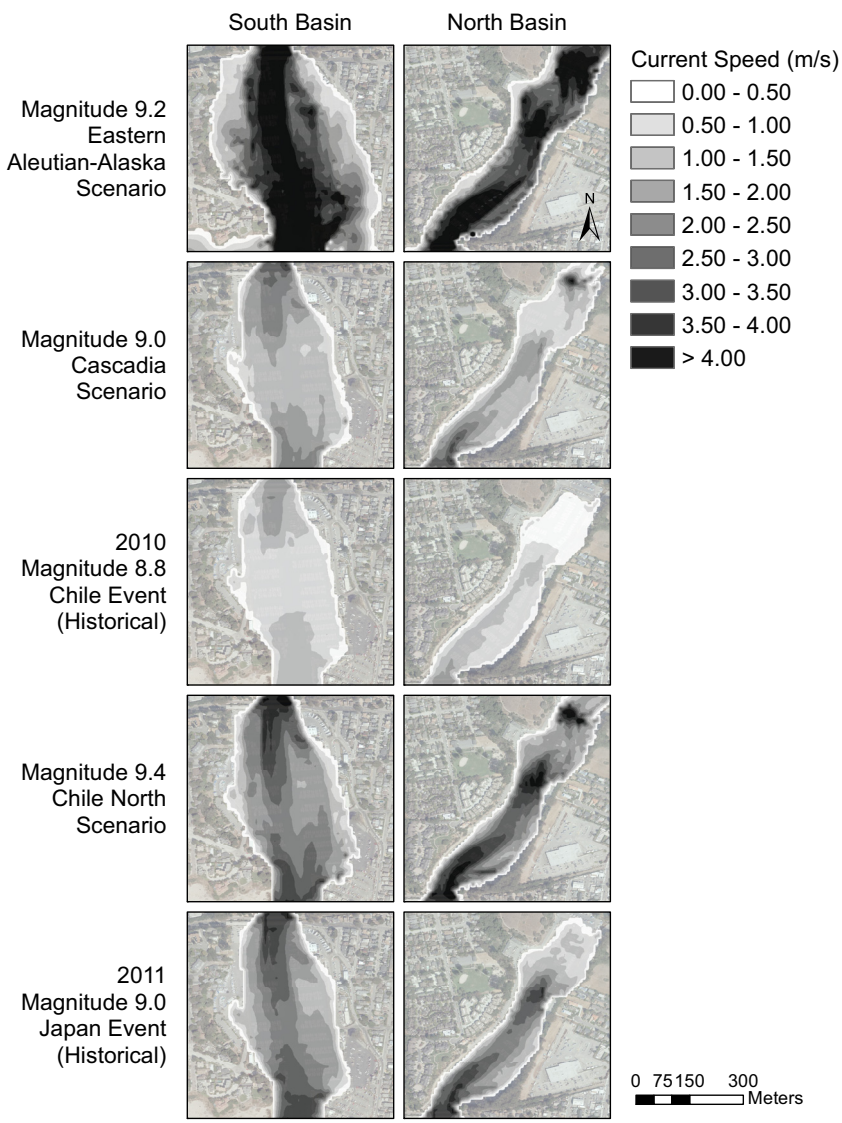

Fig. 5. Maximum modeled current speeds within Santa Cruz's south and north harbors for the magnitude 9.2 Eastern Aleutian-Alaska scenario, the magnitude 9.0 Cascadia scenario, the 2010 magnitude 8.8 Chile event (historical), the magnitude 9.4 Chile North scenario, and the 2011 magnitude 9.0 Japan event (historical), respectively (background images courtesy of United States Geological Service)

J. Waterway, Port, Coastal, Ocean Eng., 2017, 143(4): -1--1

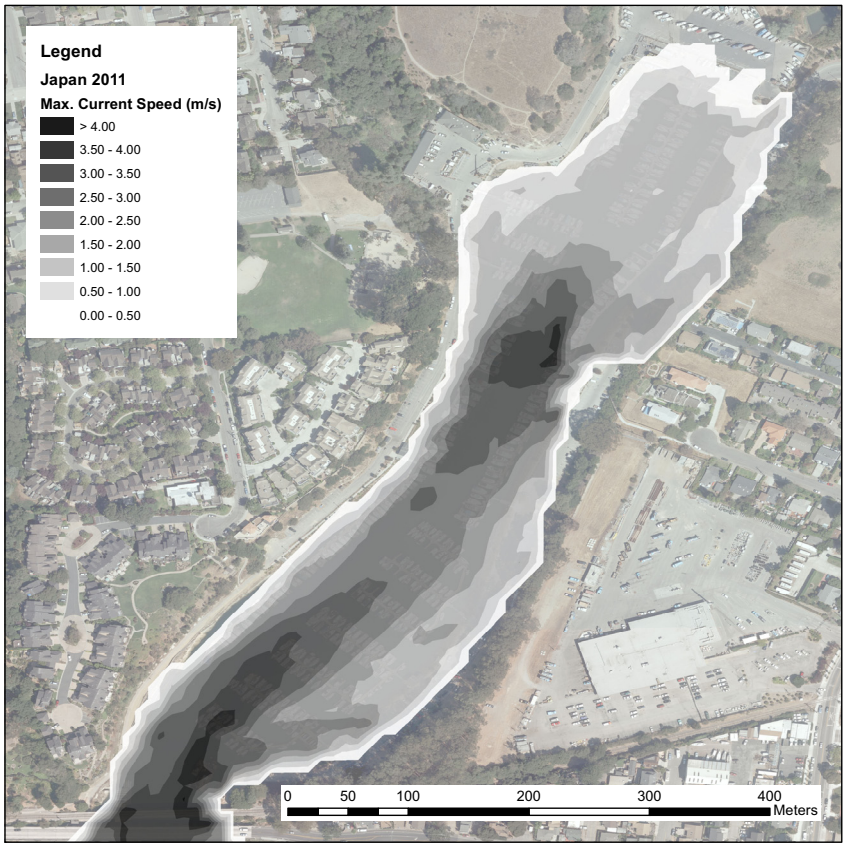

(a)

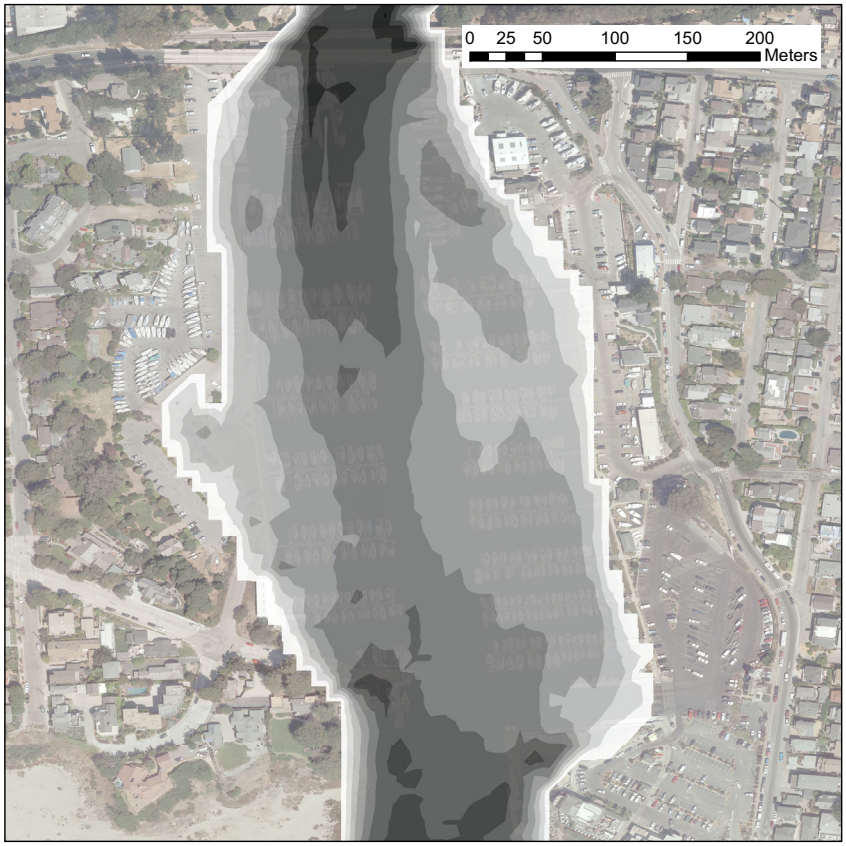

(b)

Fig. 6. Maximum modeled current speed within Santa Cruz's (a) north and (b) south harbors for the 2011 Tōhoku tsunami event (background images courtesy of United States Geological Service)

Japan event and the 9.2 Eastern Aleutian-Alaska scenario, are analyzed here. The 2011 magnitude 9.0 Japan event was selected as the primary event because of the amount of damage caused by that event and the documentation available to validate the methodologies. The 9.2 Eastern Aleutian-Alaska scenario was selected as a second event because of the potential impact of that event on the harbor. This event would produce the strongest current velocities in the harbor of any of the modeled events.

Tōhoku, Japan, (2011) Tsunami

The 2011 Tōhoku earthquake was a magnitude 9.0 that occurred on March 11, 2011. The epicenter of the earthquake was approximately 70 km east of the Oshika Peninsula of Tōhoku. The nature of the seismic event generated a powerful tsunami the impacts of which were felt throughout the Pacific Basin. In the far field, many ports, harbors, and maritime facilities along the U.S. West Coast were adversely affected by surges and currents induced by the 2011 Tōhoku tsunami (Wilson et al. 2013; Wilson et al. 2012).

The tsunami reached Santa Cruz approximately10 hours after the seismic event, creating strong currents within the harbor. Santa Cruz Harbor experienced strong currents starting the morning of March 11, 2011, continuing through to the afternoon of March 12, 2011. There were no measured currents available within the harbor; however, eyewitness reports and post-event video analysis indicated current speeds of up to 4 m/s as the tsunami entered the harbor (Ewing 2011) and maximum current speeds within the harbor of 5–7 m/s just north of the two central bridges that separate the north and south harbor (Wilson et al. 2013).

Source terms for the 2011 Tōhoku tsunami were taken from Shao et al. (2011). Modeled maximum current speeds for Santa Cruz's north and south harbors are shown in Fig. 6. The model results show significant heterogeneity in the current field with the strongest currents occurring at the harbor entrance and in the channel transition from the south to north harbor. The model results also agree reasonably well with maximum observed current speed being on the order of 3.5 m/s.

A summary of vessel, tsunami, and oceanographic characteristics used as input to the Monte Carlo analysis is provided in Table 1. Dock dimensions are not included because these parameters are deterministic and scale with the mean vessel parameters. Additionally, vessels on the ends of the docks were limited to the size that fits within the slips. Ultimately this method attempts to identify high yet average pulling forces on the dock, which are important to identifying vulnerability.

Alaska-Aleutian Tsunami

Over the last century, five large earthquakes have occurred along the AASZ. The 1964 Alaskan earthquake (magnitude 9.2) was one of these and generated a tsunami that caused significant damage along the California coast. Hence, AASZ is a crucial source region for California that has to be taken into account in a tsunami hazard assessment. The hypothetical tsunami scenario considered in this study is a variation of the 1964 earthquake, but it is located to the west of the 1964 rupture. The estimated rupture area is 700 km long and 100 km wide, and has an average slip of 25 m, which corresponds to a magnitude 9.2 earthquake. Source terms for this event were developed by Barberopoulou et al. (2011).

Maximum current speed for the AASZ event in Santa Cruz North and South Harbor are shown in Fig. 7. Model results of the Alaska-Aleutian event show significantly stronger current speeds compared with the Tōhoku event. This increase can largely be correlated with the difference in size of the tsunami's amplitude. Compared with the Tōhoku event, model results show that inundation form the Alaska-Aleutian tsunami extend well beyond the banks of the Santa Cruz Harbor, permitting more water volume to enter the harbor, and creating stronger currents within the harbor. This suggests that damage from this type of event would not only be isolated to the harbor basins but could extend landward to expand the damage footprint.

A summary of vessel, tsunami, and oceanographic characteristics used as input for the Monte Carlo analysis are provided in Table 2. Like the 2011 Japan event, dock dimensions are not included because these parameters are deterministic and scale with the mean vessel parameters. Additionally, slips on the ends of the docks were limited to the size that fits within the adjacent slips to identify high yet average pulling forces on the dock, which are important to identifying vulnerability.

Post-Tsunami Damage Assessment

After the 2011 Tōhoku tsunami event, the Santa Cruz Port District hired Mesiti-Miller Engineering, Inc. to conduct a damage evaluation of all fixed and floating facilities for the small craft harbor. The assessment consisted of a visual assessment of all floating facilities supported by guide piles; fixed structures within Santa Cruz were not included. Typical damage to the dock facilities included loose/missing flotation, cleats being pulled out from the dock, cracked whalers, and broken pile guides.

Table 1. Inputs to the Monte Carlo Fragility Analysis for the 2011 Tōhoku Tsunami Event (According to Dock)

	Vessel				Tsunami						Oceanographic	
	Length overall (m)		Maximum beam (m)		Current speed (m/s)		Current direction (degrees)		Water depth (m MSL)		Specific gravity of seawater	
Dock	Min	Max	Min	Max	Min	Max	Min	Max	Min	Max	Min	Max
N	7.6	9.1	3.0	3.7	1.0	2.0	0	5	0.7	4.7	1.025	1.040
O	9.1	9.1	3.7	3.7	1.4	1.8	0	7	1.0	4.3	1.025	1.040
W-1	7.6	7.6	3.0	3.0	1.4	2.6	0	10	1.1	3.0	1.025	1.040
W-2	7.6	7.6	3.0	3.0	1.4	2.5	2	13	1.2	2.9	1.025	1.040
W-3	7.6	7.6	3.0	3.0	1.7	2.5	8	17	1.7	3.0	1.025	1.040
J-1	9.1	9.1	3.7	3.7	1.0	1.4	13	89	0.8	3.6	1.025	1.040
U-1	9.1	9.1	3.7	3.7	2.4	3.8	1	40	1.8	4.4	1.025	1.040
U-2	9.1	9.1	3.7	3.7	1.6	3.3	0	54	0.8	3.3	1.025	1.040
V-1	9.1	9.1	3.7	3.7	1.4	3.1	5	15	1.1	3.1	1.025	1.040
V-2	9.1	9.1	3.7	3.7	1.3	2.8	0	13	1.0	3.2	1.025	1.040

Note: m MSL = meters relative to mean sea level.

J. Waterway, Port, Coastal, Ocean Eng., 2017, 143(4): -1--1

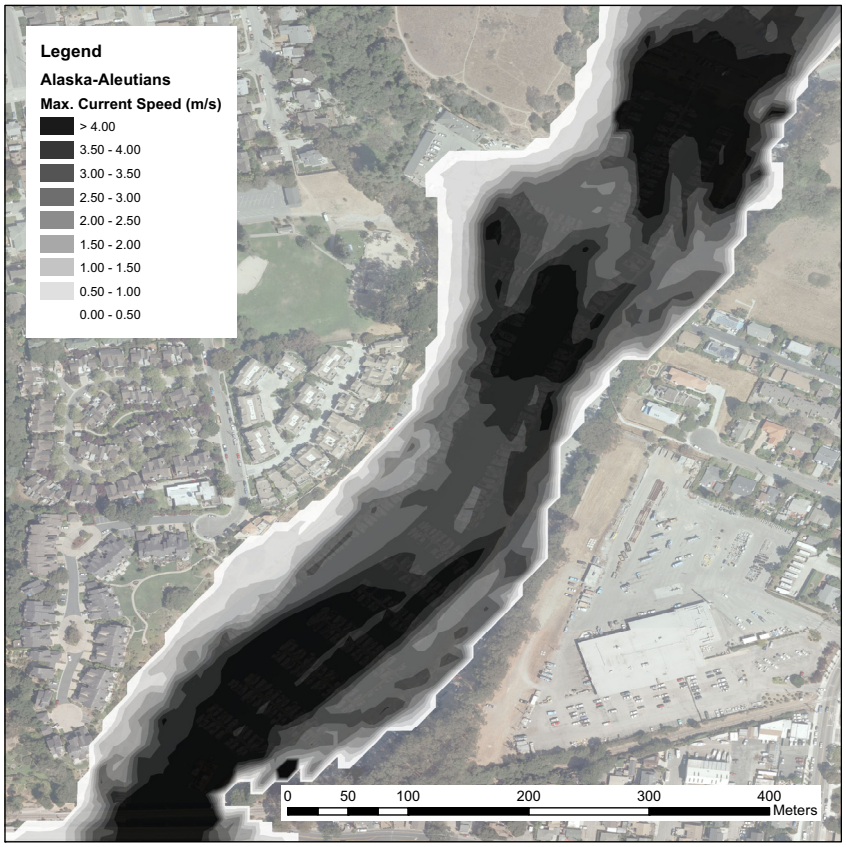

(a)

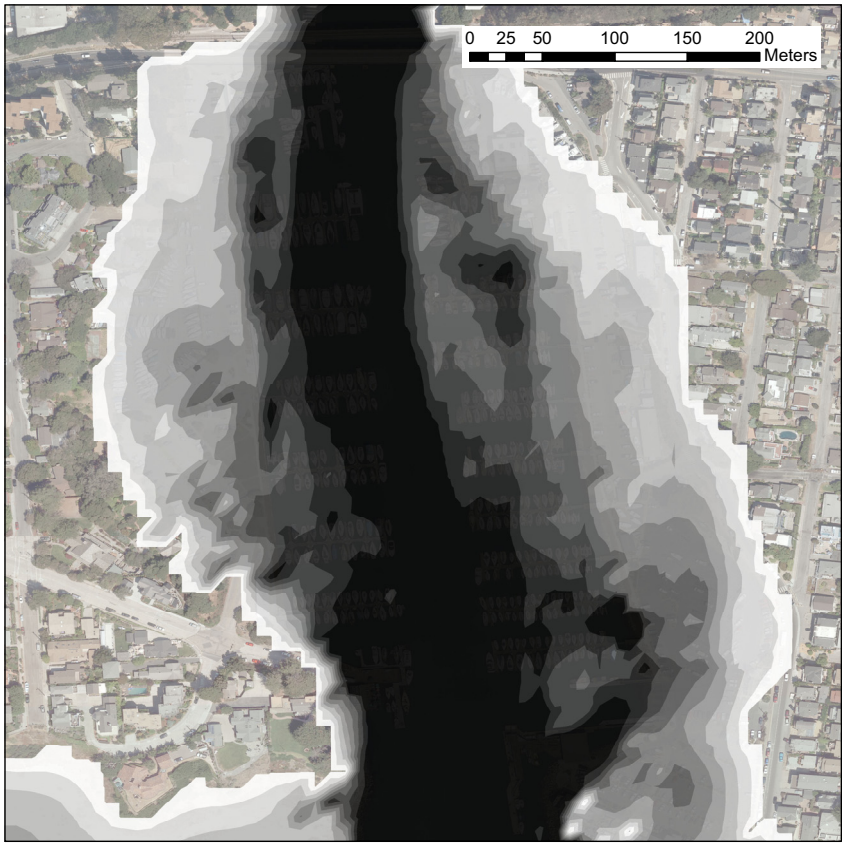

(b)

Fig. 7. Maximum modeled current speed within Santa Cruz's (a) north and (b) south harbors for the theoretical Alaska-Aleutian subduction zone tsunami event (background images courtesy of United States Geological Service)

Table 2. Inputs to the Monte Carlo Fragility Analysis for the AASZ Tsunami Event (According to Dock)

	Vessel				Tsunami						Oceanographic	
	Length overall (m)		Maximum beam (m)		Current speed (m/s)		Current direction (degrees)		Water depth (m MSL)		Specific gravity of seawater	
Dock	Min	Max	Min	Max	Min	Max	Min	Max	Min	Max	Min	Max
N	7.6	9.1	3.0	3.7	2.9	4.8	0	31	2.7	6.0	1.025	1.040
O	9.1	9.1	3.7	3.7	2.8	4.4	1	17	2.8	5.8	1.025	1.040
W-1	7.6	7.6	3.0	3.0	2.5	4.5	2	63	2.2	4.1	1.025	1.040
W-2	7.6	7.6	3.0	3.0	2.5	4.7	1	63	2.3	4.0	1.025	1.040
W-3	7.6	7.6	3.0	3.0	3.1	4.5	1	34	2.8	4.1	1.025	1.040
J-1	9.1	9.1	3.7	3.7	2.4	6.7	40	88	2.3	4.9	1.025	1.040
U-1	9.1	9.1	3.7	3.7	3.7	5.0	1	27	2.6	5.6	1.025	1.040
U-2	9.1	9.1	3.7	3.7	2.5	4.9	0	62	1.3	4.4	1.025	1.040
V-1	9.1	9.1	3.7	3.7	2.7	5.3	0	40	2.1	4.2	1.025	1.040
V-2	9.1	9.1	3.7	3.7	2.5	5.0	3	73	2.1	4.3	1.025	1.040

Note: m MSL = meters relative to mean sea level.

There are two components in a floating dock system primarily believed to cause damage within the harbor: cleat and pile guide failure. Cleat and line failure are primarily responsible for boats coming loose during tsunami events. Post-tsunami photographs taken by Mesiti-Miller Engineering, Inc. show sections of the dock in which the cleats were ripped from their mountings with only small sections of the bolts remaining. Less common are indications of lines breaking most likely because sections of lines that remain after the tsunami can be removed by the occupants and replaced.

Incidents of pile guide failure have been documented by Dengler et al (2009) in Crescent City Harbor during a post-tsunami damage assessment of the 2006 Kuril event. Dengler et al. (2009) attributed pile guide failure to the strong currents pinning the pile guides against the pilings and the guides being unable to adjust to the rising water level, which leads to failure. Because the nature of this event is somewhat difficult to analyze deterministically, this failure mechanism will be addressed probabilistically in later iterations of the model.

Post-tsunami photographs by Mesiti-Miller Engineering, Inc. support a second tension failure mechanism in which tension from the pile guides pulling against the piles led to the guides being torn from their mounting in the dock. What the photos show are areas along the floating dock in which the pile guides are disconnected from the dock without any evidence of whalers (or other dock components) being crushed.

Mesiti-Miller Engineering, Inc. gave each dock within Santa Cruz a rating from A to F, with A representing little/no damage and F representing complete failure. From this assessment, they concluded that every floating dock suffered some degree of damage (Mesiti-Miller Engineering, Inc. 2011). The ratings they developed were further used to develop low, medium, and high damage ratings for each dock within Santa Cruz Harbor. The low category corresponds to a rating from A–B, the medium category corresponds to rating from C–D, and high category corresponds to a rating of F. A polygon representing the boundaries of each dock was estimated from USGS aerial images then color coded with the corresponding damage level. The result is a spatial map of damage within north and south Santa Cruz Harbor (Fig. 8).

The north harbor sustained the most severe damage during the tsunami event. The damage within the basin, however, was spatially heterogeneous with some areas experiencing little or no impact, whereas other docks were destroyed. Docks W-1, W-2, and W-3 sustained no damage during the tsunami event and are shown in light gray. Docks U-1, U-2, V-1, and V-2 sustained a high degree of damage and are shown in black. Eyewitness accounts have indicated that damage at these docks occurred early in the tsunami event. Docks H, I-1, and I-2 also sustained a high degree of damage. However, these docks were damaged by debris that had accumulated within the harbor as a result of the initial waves. This type of damage is considered beyond the scope of this study.

Most of the south harbor sustained moderate damage during the tsunami event. The exception to this would be Dock AA, the fuel dock, and the launch ramp, which were not damaged during the event. This is likely because these are fixed structures, not floating docks like the rest of the harbor. Mesiti-Miller Engineering, Inc. attributes the difference in damage between the two harbors to the differences in infrastructure ages between the north and south basin.

Post-Tsunami Hazard Assessment

A hindcast assessment of the 2011 tsunami event and predictive assessment of the hypothetical Alaska-Aleutian event was conducted using the methodology outlined in previous sections. Current speeds and directions from each event were taken from the model results. One key weakness of this analysis is that the capacities of each component prior to the 2011 event were not known. Therefore, each fragility curve is given in terms of the required capacity for damage to occur. The output capacities can be correlated with the event damage from the previous section. The curves can be used to infer component capacities and then be used by engineers to assess under what scenarios damage to a harbor could occur. Only a limited number of docks were analyzed to validate the methodology with docks selected based on the characteristics of the flow field, dock location within the harbor, and layout.

Pile Guides

Fragility curves for pile guides from the Monte Carlo analysis are presented in Fig. 9. The results are presented with respect to the required capacity, which can be interpreted as the capacity needed to resist the tsunami demand. The scatter plot in the bottom panel corresponds to the 95% confidence level of each fragility curve by dock, or the capacity that one can state with 95% confidence would lead to a component failure for the particular tsunami scenario.

In this figure, fragility curves correspond to low, medium, and high levels of damage, as taken from the damage report, for the 2011 Tōhoku event. Assuming that all pile guides have the same structural capacity, the Monte Carlo results should show an

J. Waterway, Port, Coastal, Ocean Eng., 2017, 143(4): -1--1

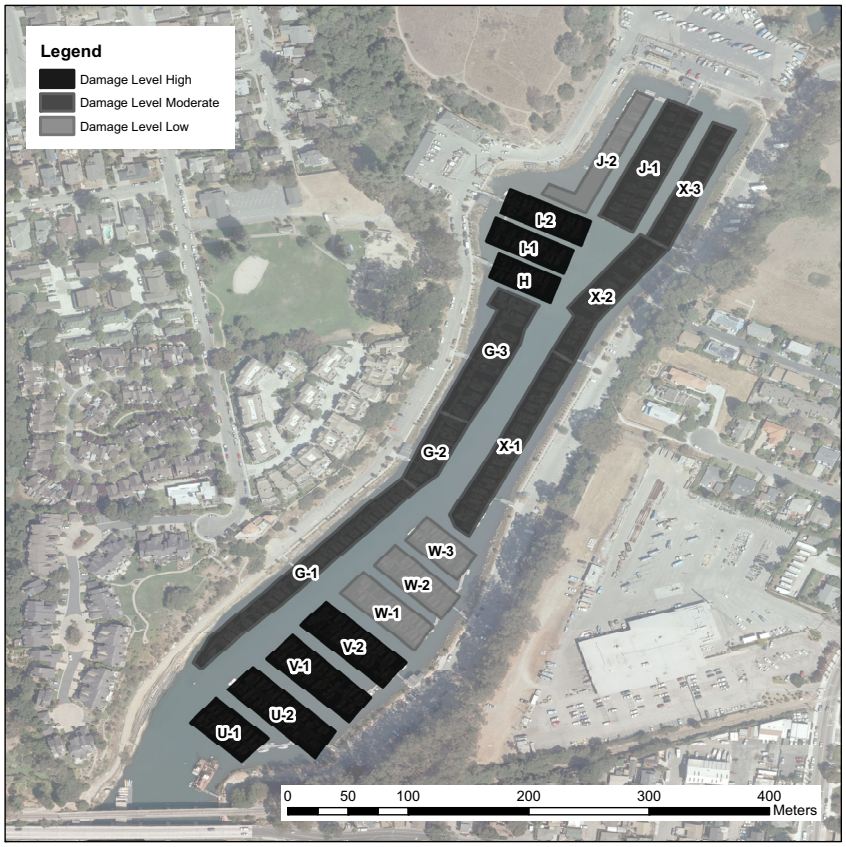

(a)

(b)

Fig. 8. Damage survey of the Santa Cruz Harbor (a) north and (b) south basins showing areas of high, medium, and low slip damage (background images courtesy of United States Geological Service)

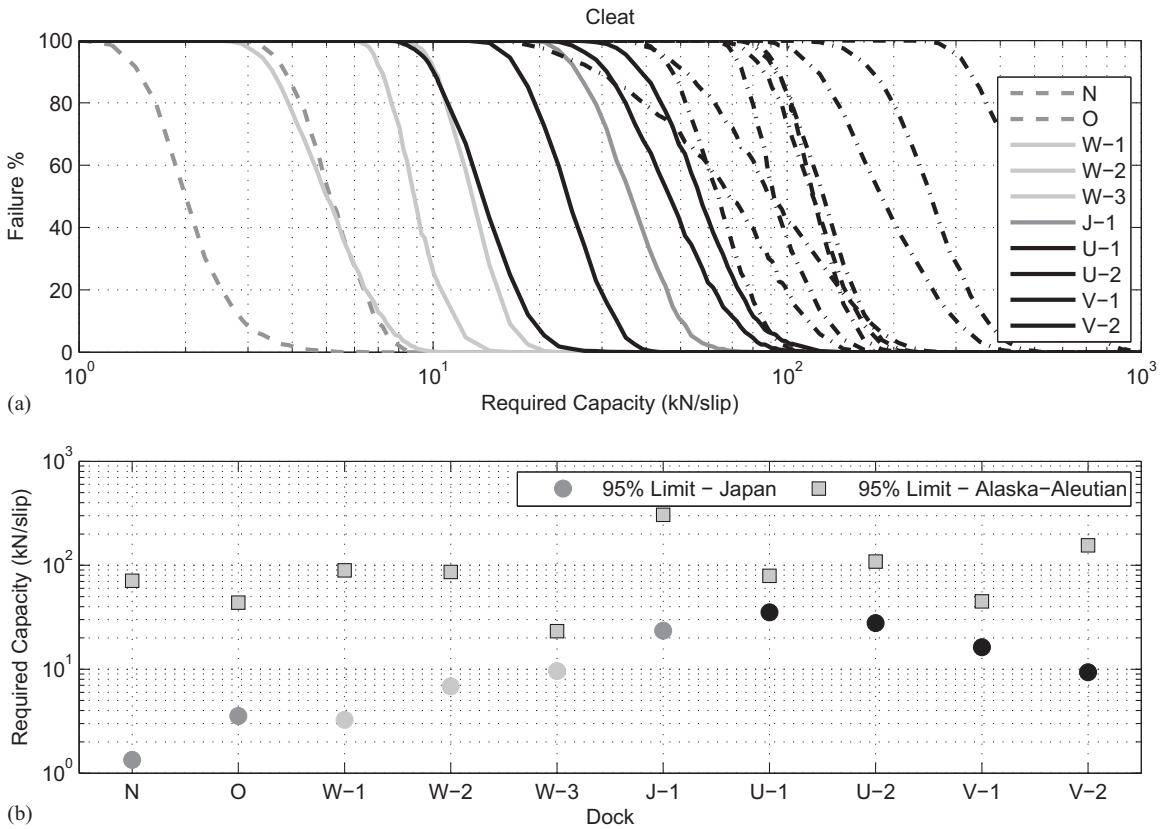

Fig. 9. Fragility curves for pile guides in Santa Cruz Harbor for the (a) 2011 Tōhoku event and Alaska-Aleutian event and (b) fragility curve 95% confidence limits for the 2011 Tōhoku and Alaska-Aleutian events (Note: Light-gray, medium-gray, and black fragility curves and markers correspond to low, medium, and high levels of observed damage for the 2011 Tōhoku event, and dash-dotted curves and multitone markers are for the Alaska event)

increasing trend for required capacity from light gray to medium gray to black. The reason for this expectation is that, if all components have the same structural capacity, those components that were not damaged (light-gray curves) should have needed a relatively small required capacity to prevent failure, or equivalently experienced a relatively small demand. Conversely, those components that were damaged (black curves) should have needed a relatively large capacity (a capacity beyond the structural capacity) to prevent failure. However, the results show a noticeable difference between the north (solid lines) and south (dashed lines) basins. The difference in the capacities required to resist failure of the south basin are significantly less than those of the north. This can be attributed to the difference in age of the two basins. With the south being finished in approximately 1962 and being constructed of mostly wood, whereas the north was finished in approximately 1973 and was constructed of mostly composite, the results indicate that the capacity of the wood docks was likely less than the composite docks. This result highlights the need to understand (or at the very least have means to differentiate) the underlying structural capacity of the system independent of the system demand.

Focusing just on the north basin, these results also show three distinct regimes in line with low, medium, and high levels of damage from the post-tsunami survey. These can be used to see when and where the transition from no damage to damage could be. For instance, the results for Docks J-1 and W-2 had nearly the same required capacity but were classified as low and moderate levels of damage. This result would, therefore, tend to suggest that the transition between low to moderate damage is somewhere between the two results. Similarly, this implies that the structural capacity of pile guides in the north basin was also likely near the Monte Carlo–predicted required capacity of the J-1 and W-2 docks.

Results for the theoretical Alaska-Aleutian event are also presented as capacity-based fragility curves and 95% confidence limits in Fig. 9. For this scenario all of the fragility curves have higher required capacities than the Tōhoku event. This result suggests that if the Alaska-Aleutian event were to occur, all of the Santa Cruz Harbor would be severely damaged by the event. If a smaller event were to be modeled, engineers could use the result to assess which docks are vulnerable to the deterministic event, therefore, helping to identify where rehabilitation efforts are best focused.

The results of the pile guide analysis highlight the skill of the Monte Carlo methodology to predict tsunami damage within a small craft harbor. When coupled with a damage report, the method was able to predict the grouping of areas of high, medium, and low damage as well as differentiate between underlying structural capacities of the north and south basin. Once calibrated, fragility curves for other events (such as the Alaska-Aleutian event) can be developed and used by engineers to determine the capacity required to withstand the design event.

Cleats

Fragility curves for cleats from the Monte Carlo analysis are presented in Fig. 10 with the results presented with respect to the required capacity. The results indicate, like the pile guide analysis, a distinct difference between the north (solid) and south (dashed)

J. Waterway, Port, Coastal, Ocean Eng., 2017, 143(4): -1--1

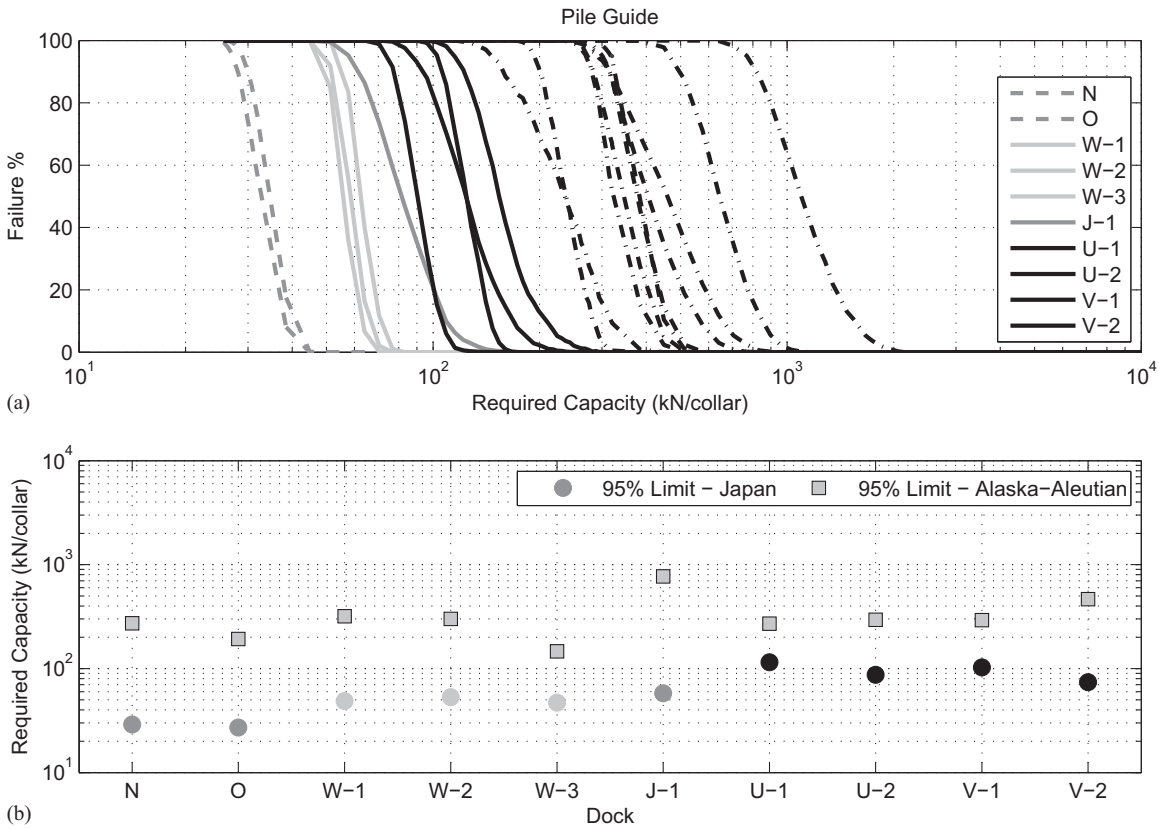

Fig. 10. Fragility curves for cleats in Santa Cruz Harbor for the (a) 2011 Tōhoku and Alaska-Aleutian events and (b) fragility curve 95% confidence limits for the 2011 Tōhoku and Alaska-Aleutian events (Note: Light-gray, medium-gray, and black fragility curves and markers correspond to low, medium, and high levels of observed damage for the 2011 Tōhoku event, and dash-dotted curves and multitone markers are for the Alaska event)

basins. However, focusing on the north basin only, the cleat results show some difference in ordering between the medium and high damage levels compared with the pile guide analysis. The Monte Carlo analysis would suggest that Dock J-1 should have experienced relatively severe cleat damage (instead of the observed moderate damage) or that Docks V-1 and V-2 experienced moderate cleat damage (instead of the observed severe damage).

One issue with the damage reports provided by Mesiti-Miller Engineers, Inc. is that the reports do not provide enough detail as to the severity of the cleat damage. The number of damaged cleats is provided for some docks (such as J-1) but not others that were completely destroyed by the tsunami (such as U-1). Therefore, only coarse interpretation of the reports can be used to draw speculative conclusions about the nature of the cleat damage. For instance, if a dock (such as U-1) was completely destroyed by the tsunami event it is reasonable to assume that some of the cleats also were destroyed. Because of this, the conclusions with respect to cleat damage cannot be as strong as the pile guide damage. The results do highlight the applicability of the method to help engineers estimate in a global sense how damage can be dispersed across the basin. Additionally, these results can be used to identify where within a harbor vessels are likely to break free from their mooring lines and become adrift, float on shore with or without the dock, or sink.

Discussion

The results of the Monte Carlo analysis highlight the methodology's ability to predict tsunami damage within a small craft harbor. Primary inputs to the Monte Carlo analysis are current speed, current direction, vessel/dock dimensions, and the underlying structural capacity of the dock. Using the results of the Monte Carlo analysis mean estimates, the current speed and current direction (converted to the orientation of the respective docks) were estimated and plotted as a function of damage type. This technique is also known as inverse modeling because the inputs are extracted from the results. The scatter plot is shown in Fig. 11. Light gray, medium gray, and black correspond to low, medium, and high damage, respectively. Squares represent results from the south basin, whereas circles represent results from the north basin.

The scatter plot shows that the severity of the damage is not dependent on the magnitude of maximum current speed alone. The incident current direction also plays a role in the structural damage. The results indicate that high current speeds with low incident angles as well as low current speed with high incident angles produce the flow momentum required to produce moderate to severe levels of damage.

The selection of input parameters is an important consideration and varies from author to author. Suppasri et al. (2014) found significant correlations between surface elevation, current speed, and damage. Muhari et al. (2015), on the other hand, found significant correlations between current speed, vessel size, and hull type. Results presented here suggest that current speed, current direction, vessel properties that control its drag load, and underlying structural capacity are important to the fragility analysis of small craft harbors.

Overall, the results highlight the need to develop physics-based models rather than simply relying on data-driven correlations. Even simple physical formulations, such as the drag equation, give some guidance as to which terms might be important in

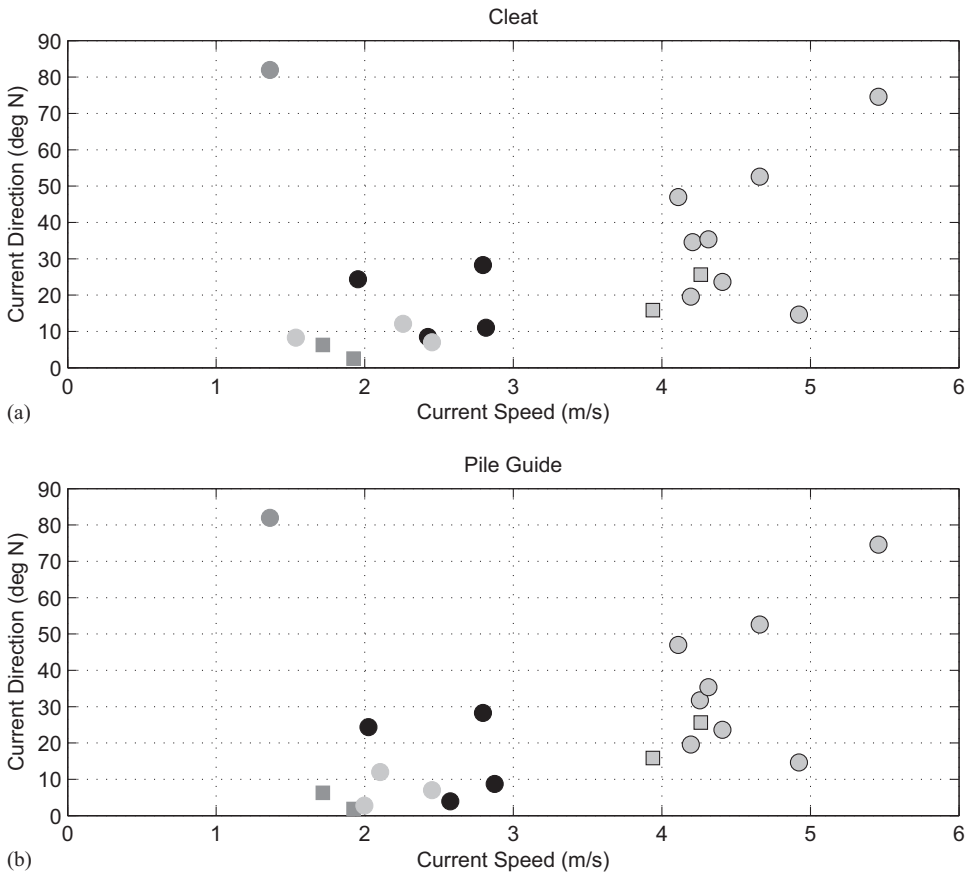

Fig. 11. Current speed and direction results for (a) cleats and (b) pile guides for the 95% confidence limits (Note: Light-gray, medium-gray, and black markers correspond to low, medium, and high levels of observed damage for the 2011 Tōhoku event, and multitone markers are for the Alaska event; squares represent results from the south basin, and circles represent results from the north basin)

the hazard analysis. The method presented here represents one possible approach and is a first step toward a fragility-based analysis in harbors.

Conclusions

This paper outlines an assessment tool that can be used to quantify the tsunami hazard to small craft harbors. The methodology is based on the demand-to-capacity ratio of a floating dock system. The results of the analysis highlight the skill of the Monte Carlo methodology to predict tsunami damage within a small craft harbor. When coupled with a damage report, the method was able to predict the grouping of areas of high, medium, and low damage as well as differentiate between underlying structural capacities in different areas of the same harbor. Once calibrated, fragility curves for other events (such as the Alaska-Aleutian event) can be developed and used by engineers to determine the capacity required to withstand the design event. Eventually a suite of scenarios could be analyzed to determine in a probabilistic sense what the required dock capacities should be to withstand extreme events.

Acknowledgments

Primary support for this work has been provided by FEMA under a cooperative technical partnership with the State of California.

References

Barberopoulou, A., Legg, M. R., Uslu, B., and Synolakis, C. E. (2011). "Reassessing the tsunami risk in major ports and harbors of California I: San Diego." *Nat. Hazards*, 58(1), 479–496.

Borrero, J. C., Lynett, P. J., and Kalligeris, N. (2015). "Tsunami currents in ports." *Phil. Trans. R. Soc. London, Ser. A*, 373(2053), 20140372.

Dengler, L., Uslu, B., Barberopoulou, A., Yim, S. C., and Kelly, A. (2009). "The November 15, 2006 Kuril-generated tsunami in Crescent City, California." *Pure Appl. Geophys.*, 166(1), 37–53.

Ewing, L. (2011). "The Tohoku tsunami of March 11, 2011: A preliminary report on effects to the California coast and planning implications." *California Coastal Commission Memo*, California Coastal Commission, San Diego, CA.

Grothe, P. G., Taylor, L. A., Eakins, B. W., Carignan, K. S., Friday, D. Z., and Love, M. (2012). "Digital elevation models of Monterey, California: Procedures, data sources and analysis." ⟨www.ngdc.noaa.gov/dem/report/download/4470⟩ (Sep. 19, 2016).

Lynett, P. J., Borrero, J., Son, S., Wilson, R., and Miller, K. (2014). "Assessment of the tsunami-induced current hazard." *Geophys. Res. Lett.*, 41(6), 2048–2055.

Lynett, P. J., Borrero, J. C., Weiss, R., Son, S., Greer, D., and Renteria, W. (2012). "Observations and modeling of tsunami-induced currents in ports and harbors." *Earth Planet. Sci. Lett.*, 327, 68–74.

Mesiti-Miller Engineering, Inc. (2011). "Tsunami damage evaluation of all fixed and floating facilities at the Santa Cruz small craft harbor." *Consulting Rep. for the Santa Cruz Port District, MME 11118*, Santa Cruz, CA.

Muhari, A., Charvet, I., Tsuyoshi, F., Suppasri, A., and Imamura, F. (2015). "Assessment of tsunami hazards in ports and their impact on marine

vessels derived from tsunami models and the observed damage data." *Nat. Hazards*, 78(2), 1309–1328.

Okada, Y. (1985). "Surface deformation due to shear and tensile faults in a half-space." *Seismol. Soc. Am. Bull.*, 75(4), 1135–1154.

Santa Cruz Port District. (2016). "Harbor user groups. History of the harbor." ⟨http://www.santacruzharbor.org/historyOfTheHarbor.html⟩ (Sep. 19, 2016).

Shao, G., Li, X., Ji, C., and Maeda, T. (2011). "Focal mechanism and slip history of the 2011 Mw 9.1 off the Pacific coast of Tohoku Earthquake, constrained with teleseismic body and surface waves." *Earth Planets Space*, 63(7), 559–564.

Suppasri, A., Muhari, A., Futami, T., Imamura, F., and Shuto, N. (2014). "Loss functions for small marine vessels based on survey data and numerical simulation of the 2011 Great East Japan tsunami." *J. Waterway, Port, Coastal, Ocean Eng.*, 10.1061/(ASCE)WW.1943-5460.0000244, 04014018.

Titov, V., and Synolakis, C. (1998). "Numerical modeling of tidal wave runup." *J. Waterway, Port, Coastal, Ocean Eng.*, 10.1061/(ASCE)0733-950X(1998)124:4(157), 157–171.

Titov, V. V., and González, F. I. (1997). "Implementation and testing of the Method of Splitting Tsunami (MOST) model." *NOAA Tech. Memo. ERL PMEL-112*, NOAA/Pacific Marine Environmental Laboratory, Seattle.

U.S. Army Corps of Engineers. (2005). "Design: Moorings, unified facilities criteria." *UFC 4-159-03*, Washington, DC.

Wilson, R., Davenport, C., and Jaffe, B. (2012). "Sediment scour and deposition within harbors in California (USA), caused by the March 11, 2011 Tohoku-oki tsunami." *Sediment. Geol.*, 282, 228–240.

Wilson, R. I., et al. (2013). "Observations and impacts from the 2010 Chilean and 2011 Japanese tsunamis in California (USA)." *Pure Appl. Geophys.*, 170(6), 1127–1147.